



Cite this: *RSC Adv.*, 2024, 14, 27153

Bi-component sensing platform for the detection of Cd²⁺, Fe²⁺ and Fe³⁺ ions†

Jagajiban Sendh and Jubaraj B. Baruah *

The ability of *N*-(1,3-dioxo-1*H*-benzo[de]isoquinolin-2(3*H*)-yl)isonicotinamide (naphydrazide) or 2,6-pyridinedicarboxylic acid (2,6-H₂pdc) individually or as a bi-component system in distinguishing and detecting Fe³⁺ or Fe²⁺ and Cd²⁺ ions was investigated. The use of these molecules as single or bi-component analytes in absorption or emission spectroscopy studies showed that under specific conditions each had their own merits for specific purposes. UV-visible spectroscopic studies of 2,6-H₂pdc for assessing the interactions with ferrous and ferric ions showed characteristic distinctions. The detection limit for Fe³⁺ analysed through UV-visible spectroscopy using naphydrazide was 0.46 μM, whereas it was 1.28 μM using 2,6-H₂pdc. Naphydrazide together with Fe³⁺ allowed distinguishing Cd²⁺ ions from Zn²⁺ and Fe²⁺ ions. The bi-component system was useful for the selective detection of Cd²⁺ ions using fluorescence spectroscopy, with a detection limit for Cd²⁺ ions of 18.31 μM. The presence of Fe²⁺ and Cd²⁺ ions in a solution of the bi-component had resulted white-light emission. An analogous compound *N,N'*-(1,3,6,8-tetraoxobenzol[imn][3,8]phenanthroline-2,7(1*H*,3*H*,6*H*,8*H*)-diyl) diisonicotinamide (binaphydrazide) was found unsuitable for such detections. Two 2,6-pyridinedicarboxylate Fe³⁺ complexes possessing protonated naphydrazide or binaphydrazide were prepared and characterised. These complexes were also found unsuitable for the detection of the said ions in solution. Electrochemical studies with the bi-component system showed that cyclic voltammograms could distinguish Fe³⁺ or Fe²⁺ from Cd²⁺ ions.

Received 26th June 2024
Accepted 14th August 2024

DOI: 10.1039/d4ra04655b

rsc.li/rsc-advances

Introduction

Detection of naturally abundant metal ions present in water at very low concentrations has been well studied.^{1–7} Among the metal ions, iron ions are more commonly found in biological systems, soil and water. The activities of iron ions in biological systems are influenced by other essential metal ions. There are many metal ions that interfere in the detection and estimation of iron ions. For example, the presence of about 24 μg g^{−1} cadmium ions in biological systems reduces the absorption of iron ions and affect the concentration of iron ions in haemoglobin or in the kidneys.⁸ A decrease in the amount of cadmium ions in ferro-proteins present in the duodenum causes anemia.⁹ Cadmium ions can enter the human body from food, the surrounding environment or certain therapies used to treat cancer. It has been reported that zinc ions regulate the absorption of cadmium ions during biological activities.¹⁰ In general, Zn²⁺ ions interfere in the fluorescence detection of Cd²⁺

ions and *vice versa*. Fe³⁺ ions are well known to interfere in the colorimetric detection of Fe²⁺ ions.¹¹ Although large numbers of receptors are used for the detection and quantification of iron and cadmium ions (ESI Tables S3 and S4†), major challenges associated with their performance and specificity persist. The quantitative estimation of cadmium or iron ions in water or soil requires procedures that do not experience interference from other cations. Such detection/quantification processes are important to maintain human and animal health. Semi-conducting quantum dots have been widely explored for the detection of different cations with high sensitivity.^{1,2} However, there are some concerns about their practical utility owing to their difficult preparation, leaching and toxicity. Hence, small common organic, less toxic molecules have scope for suitable functionalization and for use in the detection of metal ions present in water. Among the small molecules, naphthalimide derivatives are well known for use as sensors for ions.^{3,4,12–15} The optical properties, such as aggregation-induced emission or photochemical electron-transfer processes, of naphthalimide derivatives make them sensitive sensors that can be used to detect ions at the micro-scale to nano-molar-scale concentrations.¹⁶ Beside these, chelate complexes of small organic molecules can be utilized as a masking agent to modulate optical processes for the detection of metal ions.^{17,18} A system involving *in situ*-generated protons from a chelator that could

Department of Chemistry, Indian Institute of Technology Guwahati, Guwahati-781 039, Assam, India. E-mail: juba@iitg.ac.in; Tel: +91-361-2582311

† Electronic supplementary information (ESI) available: UV-visible spectroscopic and fluorescence titrations, cyclic-voltammograms, morphology, thermogravimetry of metal complexes, bond parameters of the complexes are available. CCDC 2325870 and 2325867. For ESI and crystallographic data in CIF or other electronic format see DOI: <https://doi.org/10.1039/d4ra04655b>



influence the emission spectra of specific naphthalimide derivatives was recently reported by us.¹⁹ With such a background, the aim of this study was to construct a bi-component detection platform for the detection of iron ions in the presence of cadmium, and *vice versa*. We chose to study the bi-component platform of a pyridine-based naphthalimide fluorophore with a chelating ligand (Fig. 1A and B) for determining its ratiometric responses with different metal ions.^{20,21} The proposed solution was based on supramolecular assembly²² with the following expectations: (a) two ligands competing to bind to a metal ion or mixture of metal ions would provide avenues to study the changes in emission properties stemming from the mixed ligand polynuclear/polymeric self-assemblies (Fig. 1); (b) reversibility in the association and dissociation of a non-covalent assembly would modulate the spectral properties;²³ (c) masking a metal ion by a chelating ligand would prevent a chromophore or fluorophore from having direct contact with the metal ion. This would influence the interference of one or more metal ions in a mixture;^{17,18} (d) protons

released during chelation to the solution would influence the photo-electron transfer emission; (e) non-covalent assemblies may be amenable to Foster-resonance electron transfer.^{24–26} In the literature, 2,6-pyridinedicarboxylic acid (2,6-H₂pdc)-based functional nano-materials were used for the selective detections of ions.²⁷ The use of 2,6-H₂pdc together with naphthalimide-based ligands allowed the formation of self-assembled coordination polymers.¹⁹ Capitalising on such reports, the detection of and distinction between Cd²⁺, Fe²⁺, and Fe³⁺ ions by *N*-(1,3-dioxo-1*H*-benzo[de]isoquinolin-2(3*H*)-yl)isonicotinamide (naphydrazide) as a single-component or bi-component system with 2,6-H₂pdc (Fig. 1) using UV-visible, fluorescence, and electrochemical means are described in this article. The synthesis and characterization of two Fe³⁺-pdc (pdc = 2,6-pyridinedicarboxylate) complexes having organo-cations of naphydrazide or diprotonated *N,N'*-{1,3,6,8-tetraoxobenzo[lmn][3,8] phenanthroline 2,7(1*H*,3*H*,6*H*,8*H*)diyl}diisonicotinamide (binaphydrazide) and their roles for distinguishing different ions in solution are also presented.

Experimental section

Naphydrazide²⁸ and binaphydrazide²⁹ were synthesized according to reported procedures. UV-visible spectra were recorded on a PerkinElmer Lambda 350 UV/VIS/NIR instrument (USA). Fluorescence emission spectra were recorded at room temperature using the Horiba Jobin Yvon Fluoromax-4 spectrofluorometer (USA). Lifetime decay profiles were measured on Lifespec II and FSP 920 luminescence spectrometers (Edinburgh Instruments, UK). Powder X-ray diffraction patterns were recorded on a 9 kW powder X-ray diffraction system (Rigaku Technologies, Smartlab, Japan). Thermogravimetric analysis was performed on a Netzsch, STA 449F3 instrument (Germany) at a heating rate of 10 °C min⁻¹ under an argon atmosphere. Optical microscopic images were captured by a Zeiss optical microscope (Germany) from crystals on a glass slide. Infra-red spectra of the solid samples in the region of 400–4000 cm⁻¹ were recorded with a PerkinElmer Spectrum-Two FT-IR spectrometer (USA) using the ATR method. Cyclic voltammetry studies were performed on a Potentiostat Model CHI6044E (USA) with a three-electrode set-up dipped in a cylindrical cell with a solution of the respective compound (1 mM, 10 mL solution in DMF). A glassy carbon electrode was used as the working electrode, platinum as the counter electrode, Ag/AgNO₃ as the reference electrode, and tetrabutylammonium perchlorate (0.1 mM) as the supporting electrolyte. For measuring the UV-visible spectra, stock solutions of the naphthalimide derivative (2.0 mM in DMF), 2,6-pyridinedicarboxylic acid (20.0 mM in DMF), and different metal acetates or ferric chloride (1 mM in water) were prepared. The UV-visible studies of the solution of the single-component or bi-component system were performed in a quartz cuvette. The UV-visible titrations were performed by adding the desired amounts of the solution of the metal salt dissolved in water (1.0 mM) to such solution. After each aliquot added by a micro-pipette, each solution was stirred prior to obtaining a homogeneous solution after each addition. The fluorescence spectroscopic titrations were carried out in similar

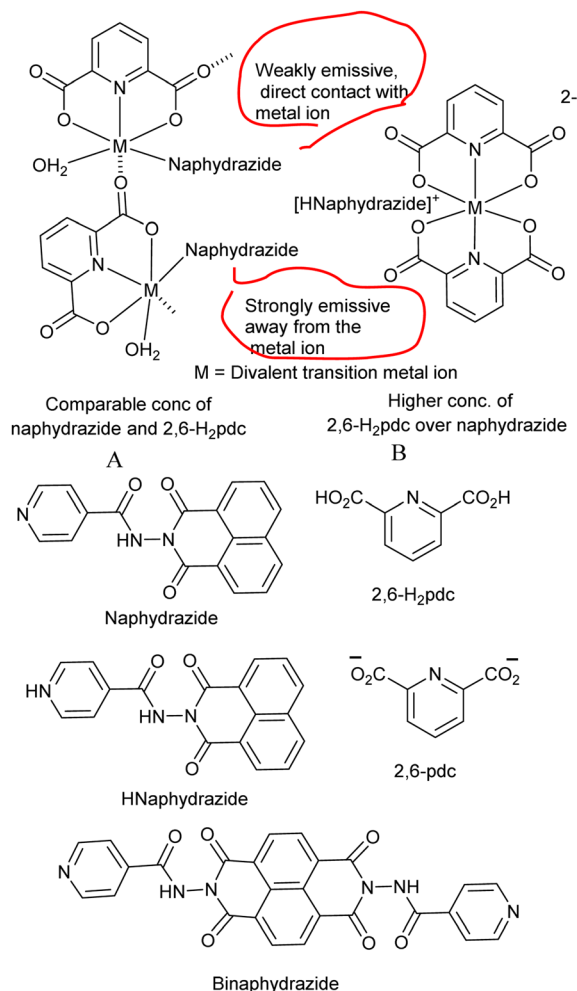


Fig. 1 (A and B) are the two proposed bi-component platforms formed by H₂26pdc and naphydrazide with a metal ion to detect another ion among various other possible assemblies, and the others are the structures of the analytes.

Table 1 Crystallographic and refinement parameters of the iron complexes

Parameters	[(Hnaphydrazide)[Fe(2,6-pdc) ₂]]·H ₂ O	[(H ₂ binaphydrazide)[Fe(2,6-pdc) ₂]]·4.5H ₂ O
Empirical formula	C ₃₂ H ₂₀ FeN ₅ O ₁₂	C ₅₄ H ₄₆ Fe ₂ N ₁₀ O ₃₁
Formula weight	722.38	1442.71
Crystal system	Triclinic	Monoclinic
<i>a</i> /Å	7.808(6)	16.017(3)
<i>b</i> /Å	14.712(11)	14.142(3)
<i>c</i> /Å	14.844(12)	26.803(6)
α /°	117.038(16)	90
β /°	92.27(2)	90.347(9)
γ /°	98.607(15)	90
<i>V</i> /Å ³	1490(2)	6071(2)
<i>Z</i>	2	4
ρ_{cal} (g cm ^{−3})	1.610	1.578
μ (mm ^{−1})	0.585	0.582
<i>F</i> (000)	738.0	2960.0
Refl. collected	35 011	71 609
Independent refl.	5296	5567
Ranges (<i>h</i> , <i>k</i> , <i>l</i>)	−9 ≤ <i>h</i> ≤ 9 −17 ≤ <i>k</i> ≤ 17 −17 ≤ <i>l</i> ≤ 17	−19 ≤ <i>h</i> ≤ 19 −16 ≤ <i>k</i> ≤ 17 −32 ≤ <i>l</i> ≤ 32
Max θ (degree)	25.204	25.409
Data/restraints/parameter	5296/0/462	5567/0/397
Goof (<i>F</i> ²)	1.067	1.045
<i>R</i> Indexes	0.0415	0.0532
[<i>I</i> > 2 σ]	0.0375	0.0404
WR ₂	0.1062	0.1258

manners. The excitation for obtaining the emission spectra was done for the naphydrazide- and binaphydrazide-containing solutions at 335 nm and 375 nm, respectively.

Determination of the detection limit

The fluorescence intensity at 400 nm of a solution of naphydrazide (2.5 mL, 2.0 mM) and 2,6-H₂pdc (400 μ L, 20.0 mM) in DMF upon the addition of different aliquots of solutions of Cd²⁺ ions (different aliquots taken from a 20 mM stock solution of water) was plotted. The detection limit was calculated by using this plot. Detection limit = $3\sigma/K$; where σ is the standard deviation of blank measurements (taken from six blank experiments) and *K* is the slope. Standard deviation of each emission reading was estimated from two independent sets of experiments by observing three sets of readings after three min intervals for each measurement (Table S5†).

Synthesis of [(Hnaphydrazide)[Fe(2,6-pdc)₂]]·H₂O. Ferric chloride (16.2 mg, 0.1 mmol) was added to a well-stirred solution of naphydrazide (31.7 mg, 0.1 mmol) and 2,6-H₂pdc (33.4 mg, 0.2 mmol, in 20 mL) in warm methanol. The reaction mixture was stirred for 3 h. A brown precipitate was formed, which was re-dissolved by adding Millipore water (10 mL). The solution was then filtered and kept undisturbed for 2–3 days for crystallization to obtain yellow crystals. Isolated yield: 70%. IR (neat, cm^{−1}): 3461 (s, $\nu_{\text{O-H}}$), 3324 (s, $\nu_{\text{amide N-H}}$), 1721 (s, $\nu_{\text{imide C=O}}$), 1635 (s, $\nu_{\text{amide C=O}}$).

Synthesis of [(H₂binaphydrazide)[Fe(2,6-pdc)₂]]·4.5H₂O. This complex was prepared by a similar procedure as for the previous compound using binaphydrazide (50.6 mg, 0.1 mmol) and 2,6-H₂pdc (66.8 mg, 0.4 mmol) and ferric chloride

(0.2 mmol, 32.4 mg). In this case, brown crystals were obtained in a 60% yield. IR (neat, cm^{−1}): 3423 (s, $\nu_{\text{amide N-H}}$), 1738 (s, $\nu_{\text{imide C=O}}$), 1640 (s, $\nu_{\text{amide C=O}}$). The complex was further characterized by XPS, thermogravimetry analysis, powder XRD, and single-crystal structure determination.

Structure determination

Single-crystal X-ray diffraction data for the complexes were collected at 297 K using Mo K α radiation (λ = 0.71073 Å) on a Bruker Nonius SMART APEX CCD diffractometer (Germany) equipped with a graphite monochromator and an Apex CCD camera. Data reductions and cell refinement were carried using SAINT and XPREP software. The structures were solved by a direct method and were refined by full-matrix least squares on *F*² using SHELXL-2018 software. All non-hydrogen atoms were refined in an anisotropic approximation against *F*² for all the reflections. Hydrogen atoms were placed at their geometrical positions according to the riding model and were refined by isotropic approximation. The crystal and structural refinement parameters are listed in Table 1.

Results and discussion

UV-visible spectroscopic study

The solution of naphydrazide in dimethylformamide (DMF) displayed a UV-absorption peak at 335 nm (ϵ = 4.51×10^{-3} mol^{−1} m²) (Fig. S1†). Upon the addition of an aqueous solution of Fe²⁺ ions to the naphydrazide solution, the intensity of the absorption at 335 nm was increased (Fig. S2†). Whereas, in a similar experiment performed by adding an aqueous solution



of Fe^{3+} ions (Fig. 2a), the absorption peak was red-shifted by 20 nm to 315 nm, and there was an increase in the intensity at this wavelength. Both showed a linear increase in the intensities with the increasing concentration of iron ions; the ratio of the two slopes from their respective plot showed the 7.90 times higher sensitivity of naphydrazide for Fe^{3+} ions over Fe^{2+} ions (Fig. 2c). A similar titration of a solution of 2,6- H_2pdc (which had an absorption peak at 270 nm and $\varepsilon = 3.67 \times 10^{-3} \text{ mol}^{-1} \text{ m}^2$) upon interaction with Fe^{2+} ions displayed an increase in the absorption intensity at 270 nm. Whereas, Fe^{3+} ions with 2,6- H_2pdc displayed two new absorption peaks at 315 nm and 360 nm. The intensities of these two absorption peaks were increased with the increasing amount of Fe^{3+} ions (Fig. S4†) added to the solution. The relative increase caused by Fe^{3+} at 315 nm with respect to that at 270 nm by Fe^{2+} was compared from the respective slopes through a linear plot of the intensity *vs.* concentration. The slope obtained from titration with Fe^{3+} was 100.46 times higher than the one from such a plot with Fe^{2+} ions. Hence, based on the relative positions as well as from the intensities of the absorptions, these two ions could be distinguished. Among the commonly used reagents, 1,10-phenanthroline³⁰ is a popular choice for the colorimetric estimation of Fe^{2+} , but in such a detection Fe^{3+} ions interfere. However, a large improvement in the detection of Fe^{2+} by 1,10-phenanthroline could be achieved by using it together with carbon dots.³¹ As there is an overlapping region for the absorption peak of the Fe^{2+} -1,10-phenanthroline complex with the emission

spectra of carbon dots, fluorescence at a longer wavelength through resonance energy transfer was observed. Selective disassembly of the bio-composites with gold nanoparticles was caused by Fe^{2+} ; which provided an avenue to detect Fe^{2+} ions without interference from Fe^{3+} ions.³² In the present case, the absorptions shown by 2,6- H_2pdc with Fe^{3+} and Fe^{2+} were distinguishable from each other.

The 2,6- H_2pdc was able to distinguish between Fe^{2+} or Fe^{3+} in solution in the presence of Cd^{2+} ions. The UV spectrum of a solution of 2,6- H_2pdc and Cd^{2+} ions upon the addition of Fe^{2+} ions showed multiple overlapping UV peaks (Fig. S3†), whereas, 2,6- H_2pdc with Fe^{3+} ions had a peak at 360 nm, and the intensity of this peak increased with increasing the concentration of Fe^{3+} ions, but was not affected by Cd^{2+} ions (Fig. S6b†). The solution of naphydrazide containing Cd^{2+} ions upon the addition of Fe^{3+} ions (Fig. 2c) showed large difference in the UV-visible spectra of the solution with Fe^{2+} ions. This was not the case with the UV spectral changes of the solution of naphydrazide containing Zn^{2+} ions upon the addition of Fe^{3+} ions. Thus, the UV-visible spectroscopic titrations of the solution of naphydrazide allowed distinguishing Fe^{2+} and Fe^{3+} in the presence of Cd^{2+} ions. The distinctions among these ions were possible due to the relative binding of 2,6- H_2pdc and naphydrazide to the corresponding metal ion, which were reflected in the individual intensity *vs.* concentration plots. Once the Zn^{2+} ions formed a complex with 2,6- H_2pdc , the Fe^{3+} ions as well as Fe^{2+} ions could not replace the zinc ion from the coordination sphere. The Fe^{3+} ions had a better binding ability to form a complex with naphydrazide than the Cd^{2+} ions. So, the enhancement of the absorption intensity at 315 nm was specifically caused by Fe^{3+} ions. There was an insignificant change in the experiments with the UV titration of naphydrazide with Cd^{2+} ions, while the similar titration with 2,6- H_2pdc showed an increase in the intensity at 335 nm (Fig. S7b†). Alternatively, Zn^{2+} and Cd^{2+} ions could be distinguished by naphydrazide in the presence of Fe^{3+} ions. An equimolar solution of naphydrazide and 2,6- H_2pdc could also distinguish between Fe^{2+} and Fe^{3+} ions. The UV-visible titration of such a solution with Fe^{2+} showed an increase in the absorption at 270 nm as well as at 335 nm. However, in the titration with Fe^{3+} ions, there were two new absorptions at 315 nm and 360 nm. These two absorption peaks were from the respective complexes of the Fe^{3+} ions with the individual components. The intensities of these peaks increased with the increasing concentration of Fe^{3+} ions. Hence, there was a distinction upon the addition of Fe^{3+} ions to the bi-component solution with respect to the individual components. The bi-component solution showed UV changes at 270 nm in the presence of different metal ions. The ratio of the slopes of the plots for the changes in intensities of the bi-component solution caused at 270 nm by Fe^{3+} with respect to that for Fe^{2+} ions was 1.70 (Fig. S5c†). So, the distinctions between the two ions by naphydrazide or the bi-component solution were similar, but it was inferior in the latter case. In the bi-component solution, there was a smoother increase at the common wavelength of 270 nm. This provided a common absorption wavelength to monitor the cations by the bi-component system. The limit of detection (LOD) for Fe^{3+} ions

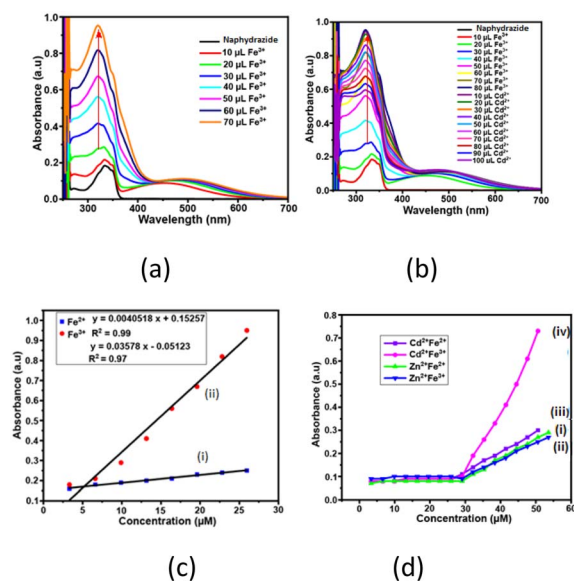


Fig. 2 UV-visible titration of naphydrazide (3.32 μM in DMF, 3 mL) with each aliquot addition of (a) Fe^{3+} ions, and (b) with different aliquots of a solution of Fe^{3+} ions, followed by the addition of Cd^{2+} ions. (c) Plots of the absorbance of solutions of naphydrazide (3 mL) with different aliquots of (i) Fe^{2+} ions at 335 nm and (ii) Fe^{3+} ions at 315 nm. (d) Plots of the intensity absorbance of solutions of naphydrazide (each 3.32 μM in DMF) at 315 nm upon addition of a solution of Zn^{2+} ions, followed by (i) Fe^{2+} or (ii) Fe^{3+} ions; Cd^{2+} ions, followed by (iii) Fe^{2+} or (iv) Fe^{3+} solution (in each titration, 10 μL stock solution from 1 mM in water of the specific metal ion was used).



by naphydrazide (determined by the changes at 315 nm) was 0.45 μM (at 315 nm), while by 2,6- H_2pdc it was 1.28 μM , and for the bi-component it was 0.09 μM . These LOD values of Fe^{3+} were within the permissible limit 0.3–0.5 mg L^{-1} of Fe^{3+} ions in drinking water recommended by the WHO.³³ Hence, the key advantage of this single-component naphydrazide or bi-component system was the ability distinguish among the three ions Fe^{2+} , Fe^{3+} , and Cd^{2+} ions and the detection of Fe^{3+} ions with a reasonable LOD, while the main limitation was that the absorptions were measured in the UV region, which is less attractive for practical applications.

Fluorescence study

Naphydrazide belongs to the family of naphthalimide, which has potential for fluorescence sensing.³⁴ It had very weak emission at 400 nm in DMF solution upon excitation at 335 nm. The emission was due to the photo-electron transfer OFF-state of the π^* to π transition.²⁸ The emission spectrum of a solution of naphydrazide at 400 nm did not change upon the addition of Cd^{2+} ions; whereas the solution of a mixture of naphydrazide and 2,6- H_2pdc in DMF showed selectively for Cd^{2+} ions, as it caused a sharp increase in the emission intensity maximum at 383 nm that appeared at a shifted peak position of 400 nm ($\lambda_{\text{ex}} = 335$ nm, Fig. 3a) for naphydrazide. Further, there was no change in the emission of the respective solution of naphydrazide and 2,6- H_2pdc in DMF upon the addition of other ions, such as NH_4^+ , Li^+ , Na^+ , K^+ , Cs^+ , Al^{3+} , Sn^{2+} , Fe^{2+} , Cd^{2+} , Zn^{2+} , or Ag^+ ions. A feeble increase in the emission intensity was caused by the addition of Ag^+ or Zn^{2+} ions to the bi-component solution. A comparison of the differences in the relative emission intensities is shown in the bar diagram in Fig. 3b. This showed that the change caused by Cd^{2+} was approximately eight times higher than the emission increase caused by Zn^{2+} ions and 3.2 times that caused by Ag^+ ions; whereas Cd^{2+} ions did not affect the emission spectrum of naphydrazide in the absence of 2,6- H_2pdc . The interferences of different ions on the emission of the bi-component solution caused by Cd^{2+} ions were also studied (Fig. 3c). From this study, it was clear that the emission of the bi-component solution was significantly affected only by Cd^{2+} ions among all the ions tested. The change in intensity was due to chelation of the cadmium ions and their subsequent protonation to cause photo-electron transfer to be turned ON.

Mixed ligand complexes of 2,6- H_2pdc with Cd^{2+} ions³⁵ with a coordination number higher than six have been reported in literature. It was reported that when forming a 2,6-pdc-complex with a metal ion by 2,6- H_2pdc , protons liberated in the solution protonated the pyridine atom of the naphydrazide to generate a PET-ON state.¹⁹ It may be mentioned that the acid-base properties of naphthalimide derivatives can help in anion detection.³⁶ On the other hand, a silver complex with naphydrazide in the solid state showed dual emission at 445 nm and 553 nm, whereas in solution it showed an aggregation-induced emission enhancement at 394 nm.²⁸ Optimization of the best ratio for obtaining the best performance by the bi-component mixture of naphydrazide with 2,6- H_2pdc in a solution containing Cd^{2+} ions (Fig. S15†) showed that a 1 : 3.2 molar ratio was

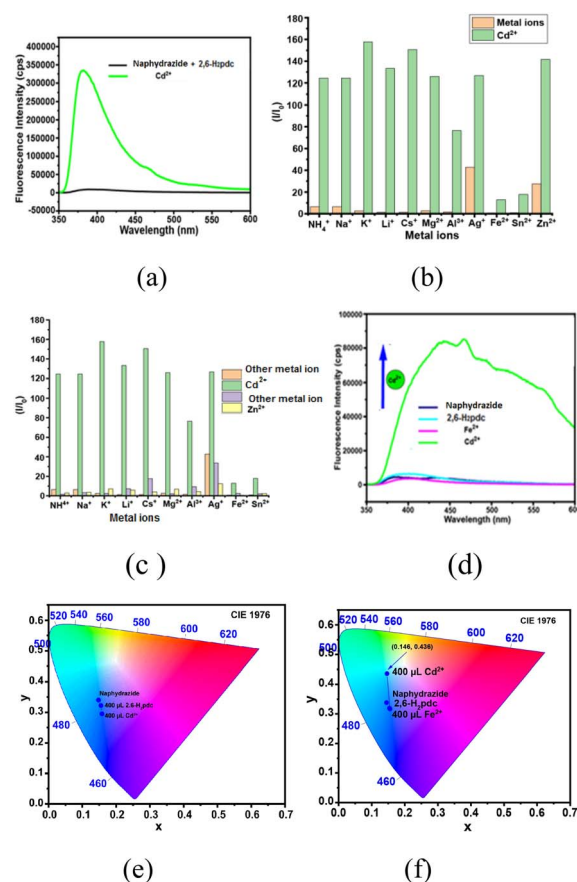


Fig. 3 (a) Fluorescence spectra ($\lambda_{\text{ex}} = 335$ nm) of a solution of naphydrazide (2 mM in DMF) together with 2,6- H_2pdc (20 mM in DMF) (i) with Cd^{2+} ions (400 μL of 20 mM in water); (ii) without Cd^{2+} ions; (b) Bar graph showing the relative changes in emission at 400 nm caused by different metal ions compared to the one caused by Cd^{2+} ions; (c) Bar graph showing the relative changes in emission intensity at 400 nm caused by different metal ions in the presence of a particular ion shown in the x-axis; (d) emission spectra showing the effect of Fe^{2+} ions on the emission spectra of a solution containing naphydrazide (2.5 mL taken from 2 mM solution in DMF) + 2,6- H_2pdc (0.4 mL taken from 20 mM in DMF) after the addition of Cd^{2+} (400 μL of 20 mM) together with Fe^{2+} (400 μL of 20 mM). (e and f) Chromaticity CIE (1976) diagram of a solution of naphydrazide and 2,6- H_2pdc with cadmium ions (2.5 mL of 2 mM, 400 μL of 20 mM 2,6- H_2pdc and 400 μL of 1 mM of Cd^{2+}) and the same solution but with Fe^{2+} ions (400 μL of 1 mM), respectively.

a suitable to study the changes in fluorescence by cadmium ions. This implied that an excess amount of 2,6- H_2pdc was required to form a bis-chelated complex (see Fig. 1B) with cadmium ions and to protonate the pyridine of naphydrazide. The addition of Fe^{3+} ions to the solution caused a quenching of the weak emission, which was expected as the role of Fe^{3+} as a quencher has been well documented.³⁷ However, when a solution of Fe^{2+} ions was added to the same solution, the emission intensity was sharply increased (Fig. 3d). These observations reflected that the Fe^{3+} ions were replacing the coordinated cadmium ions from the 2,6- H_2pdc complex, which caused a drastic change in the absorption spectrum that was not observed with the Fe^{2+} ions. In the fluorescence emission



study, we found that the Fe^{2+} ions did not inhibit the enhancement of the emission peak of the bi-component solution containing Cd^{2+} ions, but the spectral profile was changed drastically by Fe^{2+} ions, which caused a spread of the emission over wavelengths of 350 nm to 600 nm (Fig. 3d). Hence, white-light emission took place when Fe^{2+} and Cd^{2+} ions were present together in the solution of the bi-components. The effect of Fe^{2+} ions on such a solution for two different ratios of the bi-components was studied at two other ratios of 2,6- H_2pdc : naphthylazide, namely 1 : 1.25 and 1 : 2.50. At the 1 : 1.25 ratio (Fig. S10†), a broad overlapping emission from two peaks at 469 nm and 529 nm was observed, whose intensities were enhanced with the amount of Cd^{2+} ions, and finally broadened to spread over the range 390–650 nm.

Whereas with the ratio 1 : 2.50, the intensity of the broad emission peak spread over 390–650 nm increased, but at this concentration of 2,6- H_2pdc , the broad emission was skewed (Fig. S15B†), showing a maximum at 469 nm. The chromaticity indices of the two samples, one having Cd^{2+} ions and other containing both Cd^{2+} and Fe^{2+} ions together in the bi-component solution, were determined, and these are shown in Fig. 3e and f. From the chromaticity index plots, blue emission was observed from the solution of naphthylazide together with 2,6- H_2pdc in the presence of Cd^{2+} ions, but in the case of the solution having both Fe^{2+} and Cd^{2+} ions, white-light emission was observed. Due to the combined effect of f–f transition vs. $\pi^*-\pi$ transition of naphthalimide,³⁸ an europium–naphthalimide complex was reported to show white-light emission. On the other hand, certain halo-bridged cadmium coordination polymers also show white-light emission.³⁹ Here, the white-light emission observed by us upon adding Fe^{2+} ions in a bi-component solution containing Cd^{2+} ions was possibly due to a combination of PET ON and exciplex formation. The lifetime decay profile of the bi-component solution with Cd^{2+} ions displayed a bi-exponential decay profile with very short lifetimes, specifically, 0.050 ns and 0.225 ns (for the following fractions 89.58% and 10.42%), respectively. As the emission of the bi-component was poor, the lifetime without cadmium ions could not be determined. In the present case, it could be from the decay of an excited state generated by the interaction of the existing assembly of the bi-component system with Cd^{2+} ions (PET-ON state). Upon the addition of Fe^{2+} ions to the solution, the decay profile was bi-exponential and had lifetimes of 0.100 ns (fraction 27.03%) and 0.203 ns (fraction 72.97%), showing that the addition of Fe^{2+} led to an enhanced modified short-lifetime path, and a new path with a relatively higher lifetime was generated. Such, very short lifetimes have also been observed for excited state complexes of naphthalimide with organic molecules⁴⁰ and also in two photon excitations of naphthalimide, as reported in the literature.⁴¹ So, the multiple emission paths contributed to the white-light emission. A recent report suggested that white-light emission could be generated from naphthalimide derivatives.⁴²

The maximum permissible limit for Cd^{2+} ions in drinking water set by the World Health Organization is 44 μM (0.005 mg L^{-1}).³³ In the present case, the limit of detection was 18.31 μM (0.002 mg L^{-1}), which is 2.5 times more sensitive than

the required limit. This value is also comparable to many sensors reported in the literature (Table S4†), but less sensitive to several sensing molecules used for the detection of Cd^{2+} ions.^{43–48} However, those receptors had different binding mechanisms and also involved complex synthetic and pre-treatment requirements.^{43–48} In certain examples, stringent requirements for pH maintenance using a buffer were required. In the present example, a buffer was not required, and the detection could be performed in a bi-component system in DMF. Naphthalimide functionalized at the 4-position was identified as suitable for selective fluorescence ON with Cd^{2+} ions and OFF with Cu^{2+} ions.⁴⁹ This sensor had a better sensitivity than the present example towards sensing Cd^{2+} ions, but in the present case, the reported synthesis was simple, while the former involving a Schiff base also had a possibility to hydrolyze, which was absent in the present case. There are also examples of chelation-induced emission enhancement by Cd^{2+} ions on coumarin-based sensors having a higher response than Zn^{2+} ions.⁵⁰ A hydroxynaphthalene-based Schiff base showing a preference for Zn^{2+} over Cd^{2+} was also reported.⁵¹ A terpyridine-based receptor could also reportedly distinguish Cd^{2+} from Zn^{2+} in solution with a detection limit comparable to the present bi-component sensing platform, but the detection process described here could not only differentiate Cd^{2+} from Zn^{2+} , but also differentiate Fe^{2+} and Fe^{3+} ions in the presence of Cd^{2+} ions in colorimetric as well as in fluorescence detections.

Synthesis and characterization of the complexes

Naphthalimide-based complexes in general provide avenues for different π -stacking arrangements,^{52,53} and various naphthalimide-linked imidazole-based ligands forming metal complexes have been reported in the literature.⁵⁴ Also, independent reactions of naphthylazide with ferric chloride in the presence of 2,6-pyridinedicarboxylic acid could provide the complex $[(\text{Hnaphthylazide})[\text{Fe}(2,6\text{-pdc})_2]] \cdot \text{H}_2\text{O}$. This complex has an Hnaphthylazide cation and $[\text{Fe}(2,6\text{-pdc})_2]^-$ (Fig. 4a). The ferric ion in the complex is in a distorted octahedral environment and the $[\text{Fe}(2,6\text{-pdc})_2]^-$ portion of the complex displayed similar structural features to others reported in the literature⁵⁵ with different organo-cations. The metal ligand bonds are listed in Table S2.† The bulk purity of the complex was determined by comparing the experimental powder X-ray diffraction (PXRD) patterns and crystallographic information file (CIF) generated pattern (Fig. S17a†), and it was found to be a single form of the complex in the solid state. The complex was thermally unstable above 263 °C (Fig. S20a†). A similar complex $[(\text{H}_2\text{-binaphthylazide})[\text{Fe}(2,6\text{-pdc})_2]] \cdot 4.5\text{H}_2\text{O}$ was obtained by using binaphthylazide instead of naphthylazide. It had a di-protonated binaphthylazide with two $[\text{Fe}(2,6\text{-pdc})_2]^-$ anions, as shown in Fig. 4b. The asymmetric unit of the complex had half portions of the cation and one anion. In the self-assembly, the organocation $\text{H}_2\text{binaphthylazide}$ is sandwiched between the planes of 2,6- H_2pdc rings from two anions located below and above. The bond parameters of the anionic portion of the complex are listed in Table S2† and are typical of six-coordinated bis-chelated complexes. The water molecules of crystallization were highly



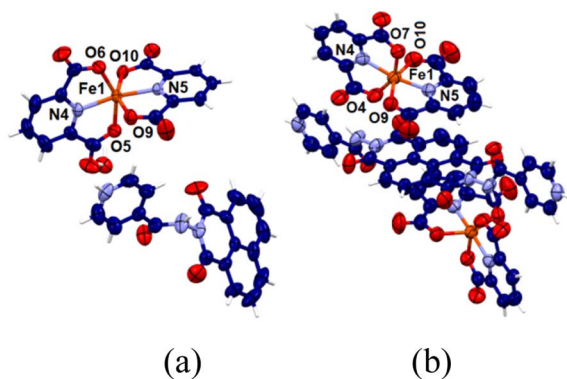


Fig. 4 Crystal structures of (a) [(Hnaphydrazide)[Fe(2,6-pdc)₂]·H₂O and (b) [(H₂binaphydrazide)[Fe(2,6-pdc)₂]·4.5H₂O (water molecules were squeezed).

disordered. As the disorder could not be resolved by X-ray diffraction data refinement, the squeeze command was applied to omit them from the structure. The purity and integrity of the composition of the complex were further confirmed by recording the PXRD pattern and matching it with one generated from the CIF file (Fig. S17b[†]). The thermogram of the compound showed weight losses due to evaporation of the four and half water molecules at 93 °C (Fig. S20b[†]). To confirm this was due to the loss of water molecules. The IR of the pristine sample of the complex was compared with a sample that was heated to 100 °C and cooled to room temperature. It was found that the O–H stretch of water molecules in the pristine sample at 3461 cm^{−1} disappeared in the sample heated prior to recording the spectrum. The complex was thermally unstable above 325 °C. A solution of [(Hnaphydrazide)[Fe(2,6-pdc)₂]·H₂O in DMF displayed UV-absorption maxima at 270 nm and 332 nm. Plots of the absorption intensity at 270 nm in different concentrations vs. concentrations of the complex in the range of 3.33–29.12 μM showed a linear increase in absorption (Fig. S21a[†]), indicating there was no aggregation of the complexes in the respective dilute solutions. This was also the same in the case of the other complex (Fig. S21b[†]). Both the complexes were non-fluorescent; hence, they were not suitable for the detection study in solution. The formation of the complexes at ambient conditions showed that the complex formation was a key step for the detection, but at a low concentration the results showed such species remained in solution.

Cyclic voltammetry study

In general, naphthalimide derivatives show two reversible redox couples⁵⁶ on the −ve side of the cyclic voltammogram (CV) due to the formation of anion radicals followed by dianions. We found that the solution of naphthylhydrazide in DMF showed such two quasi-reversible couples at $E_{1/2}$ at −0.807 and −1.321 V (Fig. S22[†]). The two redox couples for naphthylhydrazide are depicted in Fig. 5a. The complex (Hnaphydrazide)[Fe(pdc)₂]·H₂O showed quasi-reversible redox peaks at −0.418 and −0.697 V, but there was another peak at −1.02 V (Fig. S23[†]). The quasi-reversible peak at −0.418 V was attributed to the Fe²⁺/Fe³⁺

couple, whereas the $E_{1/2}$ at −0.697 V was related to anion radical formation on the protonated naphthylhydrazide. The protonated form of the Hnaphthylhydrazide in the complex had a reduction peak at a more −ve emf (volt) than the free naphthylhydrazide. The dianion formation was irreversible, so only a reduction peak at −1.02 V was observed. Cyclic voltammetric titrations performed with naphthylhydrazide by adding Fe²⁺ and Cd²⁺ ions did not show any noticeable change (Fig. S24[†]), other than a small change in the I_{pc} value. The CV bi-component solution of naphthylhydrazide with 2,6-H₂pdc showed a significant difference in the couple of the anion radical from the parent naphthylhydrazide. In this case, the radical anion generated was irreversible; whereas the couple for the dianion (Fig. 5a) remained unchanged (Fig. 5b).

Upon the addition of Fe³⁺ or Fe²⁺ ions to the solution, the reversibility for obtaining the anion radical was regained. The irreversibility conferred by 2,6-H₂pdc to the anion radical (Fig. 5c) of naphthylhydrazide was not recovered by adding Cd²⁺ ions. According to the UV-vis study, the bi-component system could clearly distinguish cadmium ions over ferric ions, so the competitive binding ability of cadmium over Fe³⁺ ions towards 2,6-H₂pdc was not the prime factor in the electrochemical process. It was the redox active ferrous or ferric ions that affected the anion radical reconversion to the neutral species. A solution of binaphthylhydrazide in DMF had two couples at $E_{1/2}$ = −0.815 V (for anion radicals) and −1.247 V (dianions). The [(H₂binaphthylhydrazide)[Fe(pdc)₂]·4.5H₂O had three redox couples with $E_{1/2}$ at −0.367, −0.766, and −1.744 V. In this case,

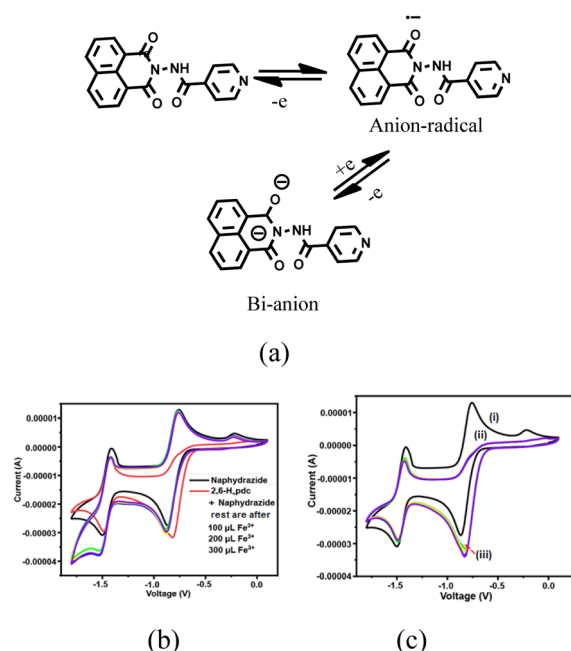


Fig. 5 (a) Redox couples of naphthylhydrazide. Cyclic voltammetric titrations: (b) (i) naphthylhydrazide and (ii) naphthylhydrazide + 2,6-H₂pdc (1 mM, 10 mL of each) in DMF to which a solution of Fe³⁺ ions was added and (c) (i) naphthylhydrazide, (ii) naphthylhydrazide + 2,6-H₂pdc, and (iii) naphthylhydrazide + 2,6-H₂pdc + Cd²⁺ ions (100 μL solution in different aliquots from a 1.0 mM solution of the corresponding stock solution of the metal ion).



the other quasi-reversible peak at -0.376 V was assigned to the ferric/ferrous couple.

Summary and conclusions

UV-visible spectroscopic studies revealed that a bi-component platform could provide a common wavelength to monitor the concentrations of Fe^{2+} and Fe^{3+} ions, while single-component systems had distinct advantages in UV studies in terms of distinguishing the ions. For example, 2,6- H_2pdc could effectively distinguish Fe^{2+} and Fe^{3+} . Naphydrazide could distinguish Fe^{3+} from Fe^{2+} in the presence of Cd^{2+} ions. In the fluorescence detection, the bi-component system was suitable for the specific detection of Cd^{2+} ions. This platform had the least interferences from many commonly abundant cations, and hence could provide a means for the useful and efficient sensing of specific ions. A comparison through UV studies on the use of naphydrazide alone or in a bi-component platform was performed and illustrated within the portions shown within the square bracket of Scheme 1. UV studies on the bi-component platform could distinguish the specific metal ions, but were not efficient enough in comparison with the specific single-component systems. The major disadvantage in the UV study was the use of shorter wavelengths.

The emission spectral changes observed with the bi-component platform were sensitive enough for the detection of Cd^{2+} ions. Chelation and the act of the photo-electron transfer ON process, followed by exciplex with different metal ions to cause or not to cause a further ON-state, were key for the

selective detection. The reversibility of the redox couple involving the anion of naphydrazide was affected by 2,6- H_2pdc , but could be regained specifically by adding Cd^{2+} ions. This strategy of ion-selective electrochemical changes has scope for the further development of electrochemical signal transduction using a particular ion with a bi-component system. The use of a bi-component platform of organic compounds with multiple metal ions to cause white-light emission has scope to modulate the intensity of UV radiation. This study provides a picture on the utility of a multi-component system from easily available compounds for influencing signal transductions through the choice of a suitable combination of components.

Data availability

The data supporting this article have been included as part of the ESI.†

Author contributions

The JS has contributed as a PhD student under the supervision of JBB and both the authors have contributed equally.

Conflicts of interest

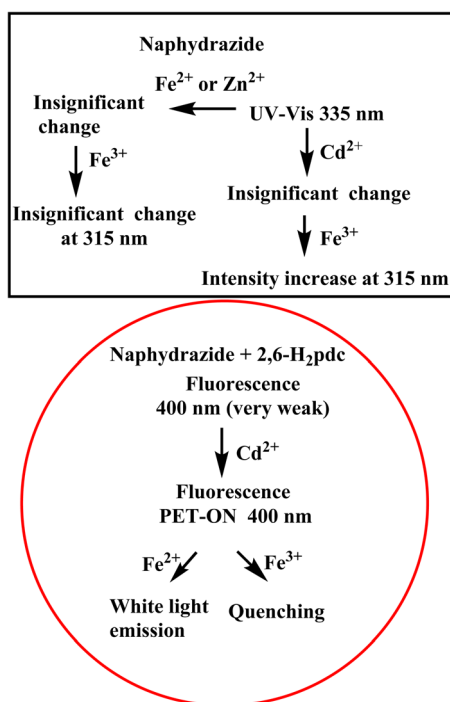
There are no conflicts of interest to declare.

Acknowledgements

The authors thank the Ministry of Human Resources and Development, New Delhi, India, (Grant No. F. No. 5-1/2014-TS.VII), Department of Science and Technology, New Delhi, India [Project no. SR/FST/CS-II/2017/23C, project No. SR/FST/ETII-071/2016(G)] and Central Instrument facilities at IIT Guwahati.

References

- 1 J. Dhariwal, G. K. Rao and D. Vaya, *RSC Sustainability*, 2024, **2**, 11–36.
- 2 M. Li, H. Gou, I. Al-Ogaidi and N. Wu, *ACS Sustain. Chem. Eng.*, 2013, **1**, 713–723.
- 3 P. Alam, N. L. C. Leung, J. Zhang, R. T. K. Kwok, J. W. Y. Lam and B. Z. Tang, *Coord. Chem. Rev.*, 2021, **429**, 213693.
- 4 F.-Y. Ye, M. Hu and Y.-S. Zheng, *Coord. Chem. Rev.*, 2023, **493**, 215328.
- 5 D. Wu, L. Chen, W. Lee, G. Ko, J. Yin and J. Yoon, *Coord. Chem. Rev.*, 2018, **354**, 74–97.
- 6 F. Zu, F. Yan, Z. Bai, J. Xu, Y. Wang, Y. Huang and X. Zhou, *Microchim. Acta*, 2017, **184**, 1899–1914.
- 7 L. M. Laglera and D. Monticelli, *Curr. Opin. Electrochem.*, 2017, **3**, 123–129.
- 8 K. Kozłowska, A. Brzozowska, J. Sulkowska and W. Roszkowski, *Nutr. Res.*, 1993, **13**, 1163–1172.
- 9 Y. Fujiwara, J.-Y. Lee, H. Banno, S. Imai, M. Tokumoto, T. Hasegawa, Y. Seko, H. Nagase and M. Satoh, *Toxicol. Lett.*, 2020, **332**, 130–139.



Scheme 1 Schematic representation of the UV-visible spectral study with naphydrazide and of the emission spectroscopy from the bi-component solution with cations.



- 10 M. M. Brzoska and J. Moniuszko-Jakoniuk, *Food Chem. Toxicol.*, 2001, **39**, 967–980.
- 11 J. Im, J. Lee, F. E. Löffler and J. Microbiological, *Methods*, 2013, **95**, 366–367.
- 12 H.-Q. Dong, T.-B. Wei, X.-Q. Ma, Q.-Y. Yang, Y.-F. Zhang, Y.-J. Sun, B.-B. Shi, H. Yao, Y.-M. Zhang and Q. Lin, *J. Mater. Chem. C*, 2020, **8**, 13501–13529.
- 13 K. Jo, S. Lee, A. Yi, T. Y. Jeon, H. H. Lee, D. Moon, D. M. Lee, J. Bae, S. T. Hong, J. Gene, S. G. Lee and H. J. Kim, *ACS Omega*, 2019, **4**, 19705–19709.
- 14 H. Xu, Y. Xiao, Y.-G. Liu and W. Sun, *Adv. Sens. Res.*, 2024, **3**, 2300032.
- 15 Q. Dong, T. B. Wei, X. Q. Ma, Q. Y. Yang, Y. F. Zhang, Y. J. Sun, B. B. Shi, H. Yao, Y. M. Zhang and Q. Lin, *J. Mater. Chem. C*, 2020, **8**, 13501.
- 16 N. Jain and N. Kaur, *Coord. Chem. Rev.*, 2022, **459**, 214454.
- 17 M. Elhabiri and A.-M. Albrecht-Gary, *Coord. Chem. Rev.*, 2008, **252**, 1079–1092.
- 18 X. Jiang, Y. Kou, J. Lu, Y. Xue, M. Wang, B. Tian and L. Tan, *J. Fluoresc.*, 2020, **30**, 301–308.
- 19 J. Sendh and J. B. Baruah, *Polyhedron*, 2024, **249**, 116792.
- 20 G. Tamil Selvan, C. Varadaraju, R. T. Selvan, I. V. M. V. Enoch and P. M. Selvakumar, *ACS Omega*, 2018, **3**, 7985–7992.
- 21 T. L. Mako, J. M. Racicot and M. Levine, Supramolecular luminescent sensors, *Chem. Rev.*, 2019, **119**, 322–477.
- 22 M. H.-Y. Chan and V. W.-W. Yam, *J. Am. Chem. Soc.*, 2022, **144**, 22805–22825.
- 23 P. Su, W. Zhang, C. Guo, H. Liu, C. Xiong, R. Tang, C. He, Z. Chen, X. Yu, H. Wang and X. Li, *J. Am. Chem. Soc.*, 2023, **145**, 18607–18622.
- 24 P. Yang, Y. Zhao, Y. Lu, Q.-Z. Xu, X.-W. Xu, L. Dong and S.-H. Yu, *ACS Nano*, 2011, **5**, 2147–2154.
- 25 C. W.-T. Chan, K. Chan and V. W.-W. Yam, *ACS Appl. Mater. Interfaces*, 2023, **15**, 25122–25133.
- 26 P.-P. Jia, L. Xu, Y.-X. Hu, W.-J. Li, X.-Q. Wang, Q.-H. Ling, X. Shi, G.-Q. Yin, X. Li, H. Sun, Y. Jiang and H.-B. Yang, *J. Am. Chem. Soc.*, 2021, **143**, 399–408.
- 27 M. L. Liu, B. B. Chen, J. H. He, C. M. Li, Y. F. Li and C. Z. Huang, *Talanta*, 2019, **191**, 443–448.
- 28 A. Tarai and J. B. Baruah, *Cryst. Growth Des.*, 2018, **18**, 456–465.
- 29 S. Bhattacharjee, B. Maiti and S. Bhattacharya, *Nanoscale*, 2016, **8**, 11224–11233.
- 30 H. Tamura, K. Goto, T. Yotsuyanagi and M. Nagayama, *Talanta*, 1974, **21**, 314–331.
- 31 X. Sun, J. Zhang, X. Wang, J. Zhao, W. Pan, G. Yu, Y. Qu and J. Wang, *Arabian J. Chem.*, 2020, **13**, 5075–5083.
- 32 P. Siyal, A. Nafady, Sirajuddin, R. Memon, S. T. H. Sherazi, J. Nisar, A. A. Siyal, M. R. Shah, S. A. Mahesar and S. Bhagat, *Spectrochim. Acta, Part A*, 2021, **254**, 119645.
- 33 World Health Organization, Avenue Appia 20, 1211 Geneva 27, Switzerland, http://www.who.int/water_sanitation_health/dwq/chemicals/cadmium/en/.
- 34 H. Xu, Y. Xiao, Y.-G. Liu and W. Sun, *Adv. Sens. Res.*, 2024, **3**, 2300032.
- 35 E. J. Gao, Y. Zhang, Z. Wen, L. Lin, L. Dai, T. D. Sun, M. C. Zhu and Y. Wang, *Russ. J. Coord. Chem.*, 2011, **37**, 887–892.
- 36 H. D. P. Ali, P. E. Kruger and T. Gunnlaugsson, *New J. Chem.*, 2008, **32**, 1153–1161.
- 37 S. Chakraborty, M. Mandal and S. Rayalu, *Inorg. Chem. Commun.*, 2020, **121**, 108189.
- 38 A. T. O'Neil, A. Chalard, J. Malmström and J. A. Kitchen, *Dalton Trans.*, 2023, **52**, 2255–2261.
- 39 Z. Qi, Y. Chen, Y. Guo, X. Yang, F.-Q. Zhang, G. Zhou and X.-M. Zhang, *J. Mater. Chem. C*, 2021, **9**, 88–94.
- 40 S. Banerjee, J. A. Kitchen, T. Gunnlaugsson and J. M. Kelly, *Org. Biomol. Chem.*, 2012, **10**, 3033–3043.
- 41 Y. Ni, L. Yang, L. Kong, C. Wang, Q. Zhang and J. Yang, *Mater. Chem. Front.*, 2022, **6**, 3522–3530.
- 42 D. C. Magri and A. A. Camilleri, *Chem. Commun.*, 2023, **59**, 4459–4462.
- 43 D. Y. Liu, J. Qi, X. Y. Liu, Z. G. Cui, H. X. Chang, J. T. Chen and G. M. Yang, *Sens. Actuators, B*, 2014, **204**, 655–658.
- 44 Y. Zhang, X. Chen, J. Liu, G. Gao, X. Zhang, S. Hou and H. Wang, *New J. Chem.*, 2018, **42**, 19245–19251.
- 45 A. Sil, A. Maity, D. Giri and S. K. Patra, *Sens. Actuators, B*, 2016, **226**, 403–411.
- 46 Y. Dai, K. Yao, J. Fu, K. Xue, L. Yang and K. Xu, *Sens. Actuators, B*, 2017, **251**, 877–884.
- 47 S. Goswami, K. Aich, S. Das, A. K. Das, A. Manna and S. Halder, *Analyst*, 2013, **138**, 1903–1907.
- 48 Y. Liu, X. Dong, J. Sun, C. Zhong, B. Li, X. You, B. Liu and Z. Liu, *Analyst*, 2012, **137**, 1837–18450.
- 49 W. Wang, Q. Wen, Y. Zhang, X. Fei, Y. Li, Q. Yang and X. Xu, *Dalton Trans.*, 2013, **42**, 1827–1833.
- 50 Shaily, A. Kumar and N. Ahmed, *New J. Chem.*, 2017, **41**, 14746–14753.
- 51 Y. Xu, H. Wang, J. Zhao, X. Yang, M. Pei, G. Zhang and Y. Zhang, *New J. Chem.*, 2019, **43**, 14320–14326.
- 52 J. K. Nath and J. B. Baruah, *Inorg. Chem. Front.*, 2014, **1**, 342–351.
- 53 D. L. Reger, E. Sirianni, J. J. Horger, M. D. Smith and R. F. Semeniuc, *Cryst. Growth Des.*, 2010, **10**, 386–393.
- 54 J. Nath, A. Mondal, A. Powell and J. B. Baruah, *Cryst. Growth Des.*, 2014, **14**, 4735–4748.
- 55 M. P. Singh and J. B. Baruah, *Inorg. Chim. Acta*, 2020, **504**, 119467.
- 56 N. Barooah, C. Tamuly and J. B. Baruah, *J. Chem. Sci.*, 2005, **117**, 117–122.

